Asian Journal of Chemistry; Vol. 32, No. 7 (2020), 1534-1542

ASIAN JOURNAL OF CHEMISTRY

https://doi.org/10.14233/ajchem.2020.22612

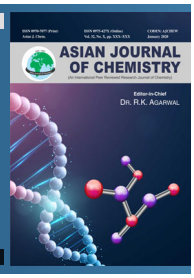

Synthesis, Characterization and Anti-Cancer Studies of Curcumin Diketimines-Heteropolyacid Composites

BHARATH SAMANNAN, JOTHI SELVAM and JEYABALAN THAVASIKANI*

Department of Chemistry, Sacred Heart College (Autonomous), Tirupattur-635601, India

*Corresponding author: E-mail: jayabalandr@gmail.com

Received: 27 December 2019; *Accepted*: 5 March 2020; *Published online*: 27 June 2020; AJC-19909

A novel composite of curcumin diketimine (CDK)-heteropolyacid (where HPA = vanadium doped Keggin anion and CDK = curcumin-benzoguanamine) had been synthesized. The hybrid composites were investigated by analytical methods such as elemental analysis, FT-IR, ^{13}C NMR, SEM, EDS, XRD, DSC-TGA, ESR spectral studies and biological activities. Encapsulated hybrid composite also studied (*in vitro*) against MCF-7 cancer cell lines. ESR results showed that the presence of (V^{4+}) ion nitrogen ligation in the composite. ^{13}C NMR of CDK ligand value of 183.37 and 55.06 ppm corresponds to (2=N) and (O-CH_3) may be due to the composites. The morphology of molybdovanadate (HPA) showed a structure of self-assembled round shape of a diameter around 1 μm.

Keywords: Curcumin diketimines, Heteropoly acid, Hybrid composites, Breast Cancer activity MCF-7.

INTRODUCTION

Curcumin is a naturally medicinal agent against cancer cells MCF-7 apoptosis *via in vitro* activity [1]. The cytotoxic effect on normal cells is minimal. *in vitro* anticancer activity and cytotoxicity chart shows the encapsulated heteropolyacid and chitosan results active apoptosis against MCF-7 cancer cell lines [2]. It aslo shows good results upon dose-dependent anticancer activity (0-100 μg). In last few years, curcumin compounds play an important role in the field of cancer treatments and various pharmacological activities, including anticancer (MCF-7), anti-inflammatory, antimicrobial and antiviral activities [3].

Non-linear polarizabilities are large due to the molecule with conjugated π-electron system [4]. In photonic applications, NLO materials are playing an effective role in wide range [5,6]. Curcumin is conjugated *via* side chain; condensation of the active group of β-diketone with various organic functional end group compounds will give a non-enolisable Knoevenagal condensate, which can effectively react with amines to form Schiff bases [7]. Curcumin is an effective anticancer agent in the breast cancer cell lines. Its bioavailability triggers finding of new approaches for increase the therapeutic efficiency [8].

Triazine derivatives play a vital role in biological activities and its functions shows of their widespread applications [9]. Triazine derivatives have been widely used as herbicides, pesticides, bactericides, anticancer drugs and enzyme inhibitors [10]. The novel curcumin compound by using Knoevenagal condensation and the composites were further examined on cancer and tumor cell lines [11]. Curcumin diketimines (CDK), synthesized *via* Knoevenagal condensation of the active double bond group of β-diketone with 2,4-diamino-6-phenyl-1, 3, 5-triazine to form *via* Schiff bases. The bioactive properties of chitosan/polyoxometalate have shown significant viability of the anticancer applications [12]. Heteropolyacid is an important compound for anti-tumor, anticancer like MCF-7 cells (breast cancer) [13]. In last few decades, transition metal doped heteropolyacid is one of the promising fields in catalyzed reaction and cancer applications [14,15].

In Keggin anion $[XM_{12}O_{40}]^{n-}$ X replace by various other transition metals in the central metal atom [16]. It is possible to compensate the negative charges in (Mo, W) ions by replacing V^{5+} as substitution of ions [17]. Transition metal substituted Keggin anions have been effective in the field of biological studies. The cytotoxicity studies of POM-entrapped caprolactam gels on SCC 131 cell lines shows 50% of cell death in

the range of 2 to 6 mM concentration in 48 h [18]. A novel studies of transition metal doped heteropolyacid (HPA) with curcumin diketimines (CDK) to form composites of [V-HPA (CDK)]. In this work, polyoxometalate was conjugated curcumin-triazines cytotoxicity studies on MCF-7 cell lines shows 86% of apoptosis or cell death with (3.12-100 μG/mL) different concentrations in 48 h. In this paper, the synthesis, characterization and anticancer activity of curcumin diketimines (CDK) -heteropolyacid composites have been discussed, where HPA = vanadium doped Keggin anion and CDK = curcumin-benzoguanamine.

EXPERIMENTAL

Synthesis of transition metal substituted heteropolyacid (HPA): Sodium molybdate (4.0 g, 2 mmol) and vanadyl sulphate (0.5 g, 1 mmol) were dissolved in the minimum amount of double distilled water. To this solution, disodium hydrogen phosphate (1.0 g, 1 mmol) dissolved in water was added with constant stirring (white to purple coloured solution). To this content, a few drops of conc. HNO_3 was added to form yellowish orange coloured precipitate composite, which was filtered and then dried at room temperature. Gravimetric analysis calcd. (found) %: Mo: 66.46 (66.27) and V: 2.94 (2.90).

Synthesis of curcumin diketimines (CDK) Schiff base: A mixture of (1*E*,6*E*)-1,7-*bis*(4-hydroxy-3-methoxyphenyl)-hepta-1,6-diene-3,5-dione (0.736 g, 1 mmol) and 2,4-diamino-6-phenyl-1,3,5-triazine (0.50 g, 2 mmol) in ethanol solution was stirred at room temperature in the presence of piperidine for a period of 6 h. The reddish yellow solid obtained was filtered and recrystallized from ethanol. The EDS analysis showed the presence of C 69.70% and O 9.59 % in the CDK ligands. The schematic synthesis route of curcumin diketimines (CDK) is shown in Fig. 1.

Synthesis of metal(II) composites: The [HPA(CDK)] complex was synthesized by the addition of hot solution of HPA (1 mmol) in ethanol (25 mL) to the hot solution of CDK (0.5 g, 1 mmol) in the same ethanol solution (25 mL). The product was refluxed for 1 h with constant stirring. The formed product was filtered and then dried at room temperature. The schematic representation of curcumin diketimines (CDK) with HPA is shown in Fig. 2. EDS analysis showed that the presence of Mo 42.90%, O 27.39%, C 19.07%, V 2.07% and P 1.21% in the composites. Gravimetric analysis calcd. %: Mo 42.97% and V 2.03%.

Characterizations: FT-IR was carried out in Shimazdu FT-IR spectrometer using KBr pellets. The morphological structure of complex was investigated using SEM (JOEL JSM 6390). X-ray diffraction were collected using Shimazdu XRD-6000, operating in Bragg-Brentano focusing geometry and using Cu$K\alpha$ radiation (λ = 1.5418 Å) from a generator operating at 40 kV and 30 mA. The electron spin resonance (ESR) spectrum was obtained through JEOL, JES FA200 instrument where the X-Band frequency: 8.75-9.65 GHz, sensitivity: 7×10^9 spins/0.1 mT, resolution: 2.35 μT and better variable temperature facility (-153 ºC to + 25 ºC).

Cell culture: MCF-7 (Breast cancer) cell lines were procured from NCCS, stock cells was cultured in medium supplemented with 10% inactivated fetal bovine serum (FBS), penicillin (100 IU/mL), streptomycin (100 μg/mL) in an humidified atmosphere of 5% CO_2 at 37 ºC until confluent. The cell was dissociated with TPVG solution (0.2% trypsin, 0.02% EDTA, 0.05% glucose in PBS). The viability of the cells were checked and centrifuged. Further 50,000 cells/well was seeded in a 96 well plate and incubated for 24 h at 37 ºC, 5% CO_2 incubator.

Cytotoxicity studies: The monolayer cell culture was trypsinized and the cell count was adjusted to 1.0×10^5 cells/mL using respective media containing 10% FBS. To each well of 96 well microtiter plate, 100 μL of diluted cell suspension (50,000 cells/well) was added. After 24 h, when a partial monolayer was formed, the supernatant was flicked off, washed the monolayer once with medium and 100 μL of different test concentrations of test drugs were added on to the partial monolayer in microtiter plates. The plates were then incubated at 37 ºC for 48 h in 5% CO_2 atmosphere. After incubation, the test solutions in the wells were discarded and 100 μL of MTT (5 mg/10 mL of MTT in PBS) was added to each well. The plates were incubated for 4 h at 37 ºC in 5% CO_2 atmosphere.

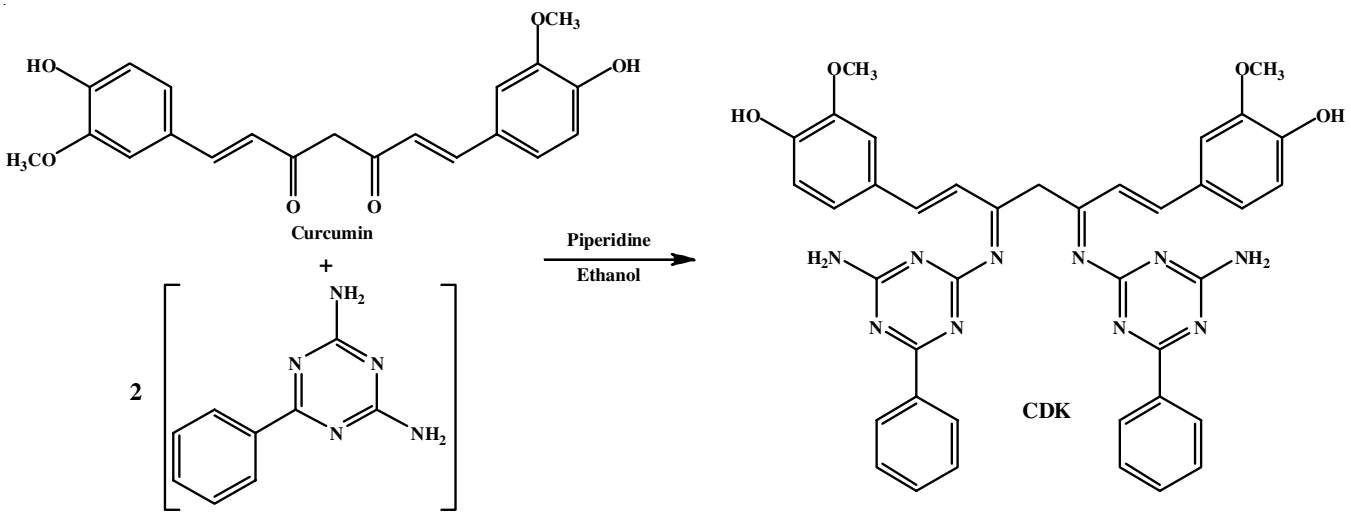

Fig. 1. Schematic representation of curcumin diketimines (CDK)

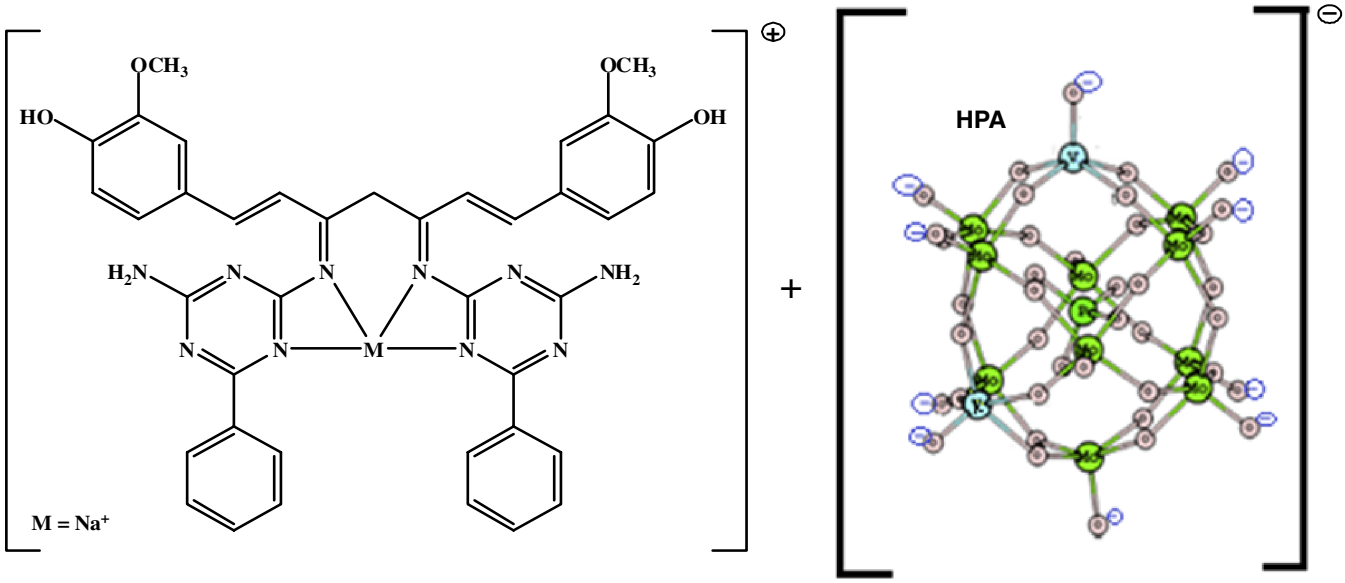

Fig. 2. Schematic representations of curcumin diketimines (CDK) with HPA

The supernatant was removed and 100 µL of DMSO was added and the plates were gently shaken to solubilize the formed formazan. The absorbance was measured using a microplate reader at a wavelength of 570 nm. The percentage growth inhibition was calculated using the following formula and concentration of test drug needed to inhibit cell growth by 50% (IC_{50}) values was generated from the dose-response curves for each cell line.

MTT assay: The *in vitro* determinations of toxic effects of unknown compounds have been performed by counting viable cells after staining with a vital dye. Alternative methods used were the measurement of radioisotope incorporation as a measure of DNA synthesis, counting by automated counters and others which rely on dyes and cellular activity. Dissolved MTT is converted to an insoluble purple formazan by cleavage of tetrazolium ring by mitochondrial dehydrogenase enzymes of viable cells. This water insoluble formazan can be solubilized using DMSO, acidified isopropanol or other solvents (pure propanol or ethanol). The resulting purple solution was spectrophotometrically measured. An increase or decrease in cell number results in a concomitant change in the amount of formazan formed, indicating the degree of cytotoxicity caused by the test material.

IC_{50} value: The IC_{50} of a drug can be determined by constructing a dose-response curve and examining the effect of different concentrations of antagonist on reversing agonist activity. IC_{50} values can be calculated for a given antagonist by determining the concentration needed to inhibit half of the maximum biological response of the agonist. The IC_{50} values for cytotoxicity tests were derived from a non-linear regression analysis (curve fit) based on sigmoid dose response curve.

RESULTS AND DISCUSSION

FT-IR analysis: In the FT-IR spectrum of HPA shows four absorbed bands of heteropolyacid at 1063, 956, 862 and 774 cm^{-1}, which are assigned to P-O, M-O (M: Mo, V), inter and intra-octahedral M-O-M stretching vibrations. The other two peaks at 3430-3400 and 1650-1600 cm^{-1} represented the presence of H_2O in the HPA. The positive shift in the vibrations of P-O and M-O peaks at 1062-1057 and 962-956 cm^{-1}, respectively confirmed the modified structure in the composites [HPA(CDK)] (*i.e.*; 5-8 cm^{-1}) is observed in Fig. 3. The CDK peaks value at 3188 and 2935 cm^{-1} were assigned to C-H aromatic stretching, one at 3514 cm^{-1} corresponds to the O-H group. The peak at 1625 cm^{-1} might be due to the primary amine (N-H bending), while the peak at 1586 cm^{-1} corresponds to N-H stretching of 3° vibration. The other peaks at 1428, 1283, 1030, and 688 cm^{-1} were assigned to the C-C aromatic ring, C=O (phenolic), C-O (OCH_3) and N-H (1° amine, out of the plane). Fig. 3 also showed the peaks at 3179 and 2932 cm^{-1} which correspond to C-H stretching, 1410 cm^{-1} (C-C aromatic stretching), 1035 cm^{-1} is assigned to C=O (OCH_3), 1278 cm^{-1} is due to C=O (phenolic), band at 1630 cm^{-1} corresponds to (C=N/ benzene

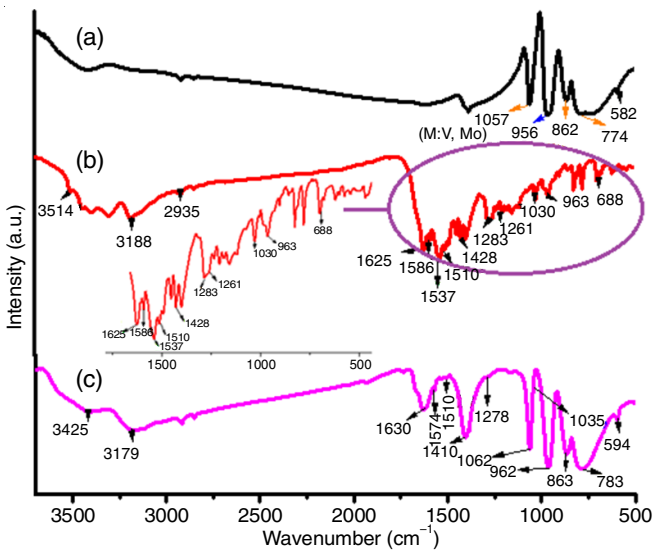

Fig. 3. FT-IR spectrum of (a) HPA (b) CDK (c) [HPA(CDK)]

ring skeleton). The other key IR spectral data of HPA, CDK and [HPA(CDK)] are listed in Table-1. The curcumin-benzoguanamine spectral data has some similar corresponding peaks, whereas the inclusion of both compounds causes disappears of the some spectral peaks of the composites.

TABLE-1
FT-IR SPECTRAL DATA (cm^{-1}) OF
(A) HPA, (B) CDK AND (C) [HPA(CDK)]

	[HPA(CDK)]	CDK	HPA
ν(O-H) phenolic	3425	3514	–
ν(C-H) aromatic ring	3179	3188	–
ν(C-H)	2932	2935	–
ν(C=N)	1630	1625	–
ν(N-H) 3° vibration	1574	1586	–
ν(C=O, C=C)	1510	1510	–
ν(C-C) aromatic ring	1410	1428	–
ν(C=O) phenolic	1278	1283	–
ν(C=O) (OCH_3)	1035	1030	–
ν(N-H) out-of-plane	687	688	–
ν(M-N)	594	–	582
ν(P-O)	1062	–	1057
ν(M-O) (M: Mo, V)	962	–	956
ν(M-O-M) inter	863	–	862
ν(M-O-M) intra	783	–	774

^{13}C NMR analysis: Fig. 4 shows that ^{13}C NMR spectral data which illustrated the curcumin-benzoguanamine (CDK) in methanol were clearly observed. In ^{13}C NMR spectrum of CDK, the resonance peak at 47 ppm is due to methanol solvent. The carbon C_{11} (OCH_3) peak at 55.060 ppm corresponds to the end methyl group of curcumin structure, while the resonance signal of carbon $C_{(2,2')}$ 2=N at 183.378 ppm is due to the inclusion of both organic compounds, $C_{(7,7')}$ at 115.497 ppm. The peak at 148.025 ppm exhibited the $C_{(8,8')}$ and $C_{(9,9')}$, while $C_{(1,1')}$ disappearance might be due to inclusion of curcumin-benzoguanamine composites [19]. Another peak at 140.74 ppm corresponds

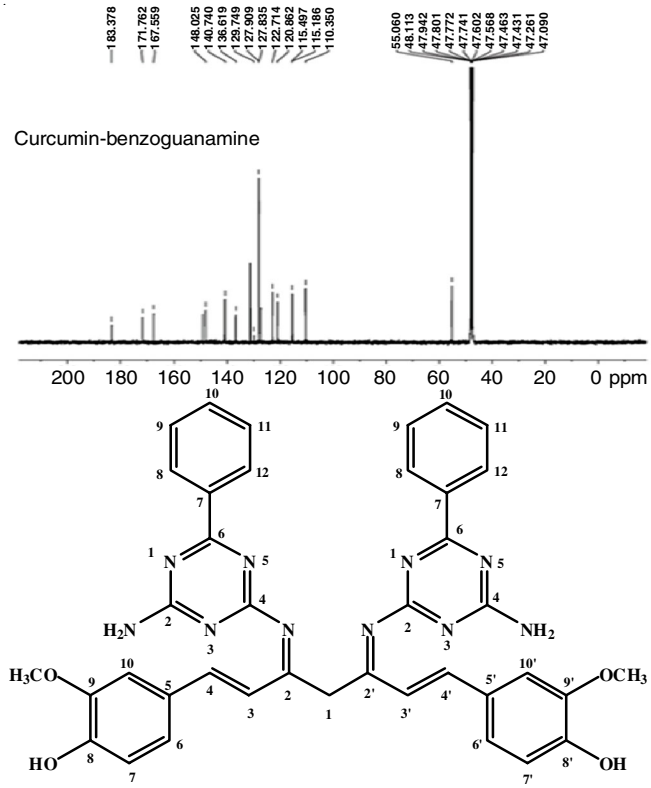

Fig. 4. ^{13}C NMR of curcumin diketimines (CDK)

to the carbon $C_{(4,4')}$. The resonance peaks shift at 127.835, 122.714, 120.862 and 110.350 ppm exhibited due to the corresponding carbon $C_{(5,5')}$, $C_{(6,6')}$, $C_{(3,3')}$ and $C_{(10,10')}$. The ^{13}C NMR spectrum of CDK (benzoguanamine) shifts of carbon groups correspond to $C_{(1,2)}$, $C_{(3)}$, $C_{(4)}$ and $C_{(5,9}/C_{6,8)}$ at 167.559, 171.762, 136.619 and 127.909 ppm are given in Table-2.

X-band EPR studies: The X-band EPR spectroscopic studies for HPA and [HPA(CDK)] revealed a hyperfine structure (VO^{2+}) in the eight line EPR signals in the composites (Fig. 5a-b). The eight line EPR signal is due to the hyperfine interaction

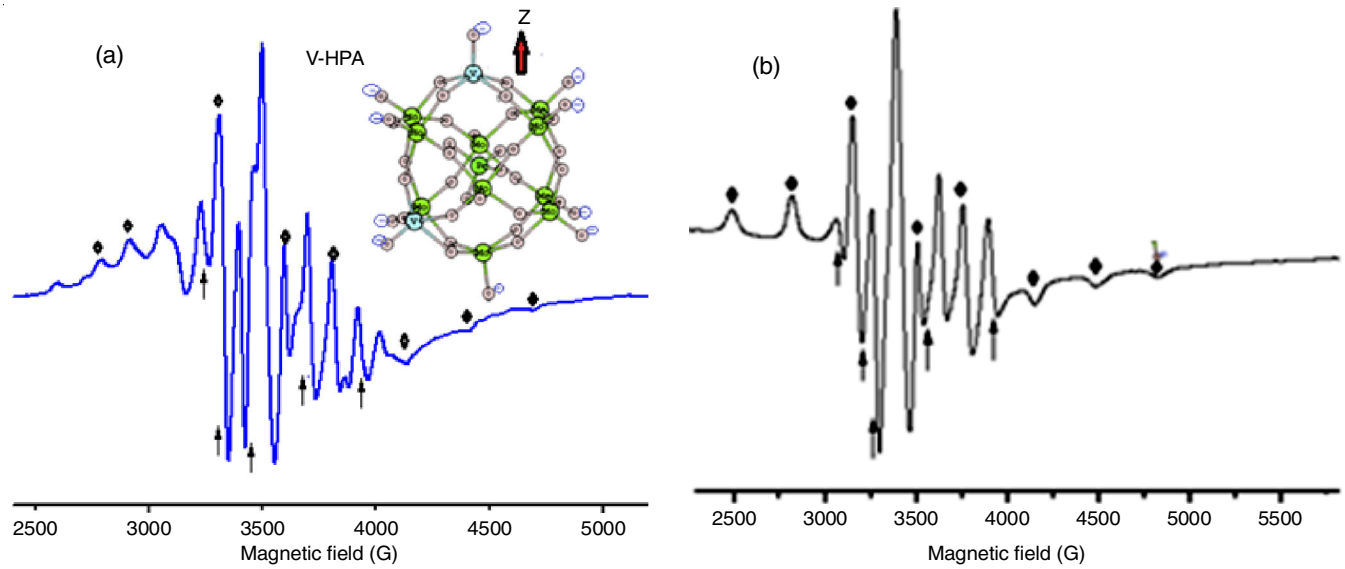

Fig. 5. EPR spectrum of (a) HPA and (b) [HPA(CDK]

TABLE-2
^{13}C NMR SPECTRAL DATA OF CDK

δ (ppm)			
Curcumin (ppm)		Benzoguanamine (ppm)	
$C_{(2,2')}$ (2=N)	183.378	$C_{1,2}$	167.559
$C_{(8,8')}$	148.025	C_3	171.762
$C_{(4,4')}$	140.740	C_4	136.619
$C_{(5,5')}$	127.835	$C_{5,9}/C_{6,8}$	127.900
$C_{(6,6')}$	122.714		
$C_{(3,3')}$	120.862		
$C_{(7,7')}$	115.497		
$C_{(10,10')}$	110.350		
$C_{(11,11')}$ (OCH_3)	55.060		

between the electron spin and the nuclear spin is due to the presence of vanadium(IV). The EPR spectral parameters of HPA and [HPA(CDK)] confirmed the presence of V^{4+} with sharp peaks in the composites (Table-3). The $g_{\|}$ and $g_{\perp}$ values of HPA were found be 1.96 and 1.94, respectively. The G values are very close to the reported in the literature [20].

TABLE-3
X-BAND EPR SPECTRAL DATA OF
(A) HPA AND (B) [HPA(CDK)]

Complex	$g_{\|}$	$g_{\perp}$	Ref.
HPA	1.96	1.94	This work
	1.95	1.98	[25]
[HPA(CDK)]	1.91	1.94	This work

Powder-XRD analysis: The XRD patterns of HPA and [HPA(CDK)] is shown in Fig. 6. The observed three strong peaks at 2θ = ~ 10º, 26º and 36º show the presence of HPA in the composites [HPA(CDK)] [21]. The diffraction peaks at 2θ = 10.6º, 15º, 21º and 62º were corresponded to the peaks of CDK and HPA in the composite [HPA(CDK)] [22]. The curcumin major peaks were observed at 2θ = 14.8º, 17.5º and 20.1º, which again confirms the presence of CDK in the [HPA(CDK)] composite [22]. The peaks at ~ 20.83º and 42.4º of benzoguamine appeared in the CDK ligands are shown in Fig. 6a. The XRD data are given in Table-4 and the characteristics peaks of HPA are matched with the JCPDS standard card (9-816) [23].

SEM/EDS analysis: The morphological structure of HPA, CDK and [HPA(CDK)] are shown in Fig. 7. Interestingly, HPA formed into a geodesic shaped like a structure of microscale. The aggregation of self-assembled HPA was round shape around

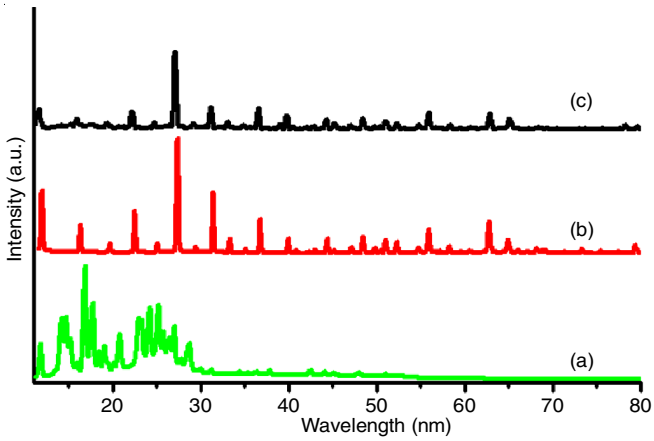

Fig. 6. XRD pattern of (a) CDK, (b) HPA (c) [HPA(CDK)]

TABLE-4
XRD SPECTRAL DATA OF (A) HPA,
(B) CDK AND (C) [HPA(CDK)]

Samples	2θ value	Grain size (nm)
HPA	10.4	34
	15.0	35
	21.2	36
	26.1	37
	36.0	37
	62.0	47
CDK	14.83	24
	17.50	19
	20.10	27
	20.80	19
	42.40	21
[HPA(CDK)]	10.68	39
	15.01	35
	20.98	32
	26.20	41
	42.46	23

~ 390-500 nm in size as shown in Fig. 7a. The heteropolyacid was self-assembled in micro-geodesic shape which is successfully achieved at a micro level. The magnified image of CDK shows a stack like nano- and micro-structure assemblies with the size ranged from 450 nm to 1 µm (Fig. 7b). The stack layer presence on the geodesic shaped which was around ~500 nm is shown in Fig. 7c. The EDS spectra of HPA, CDK and [HPA (CDK)] are shown in Fig. 8.

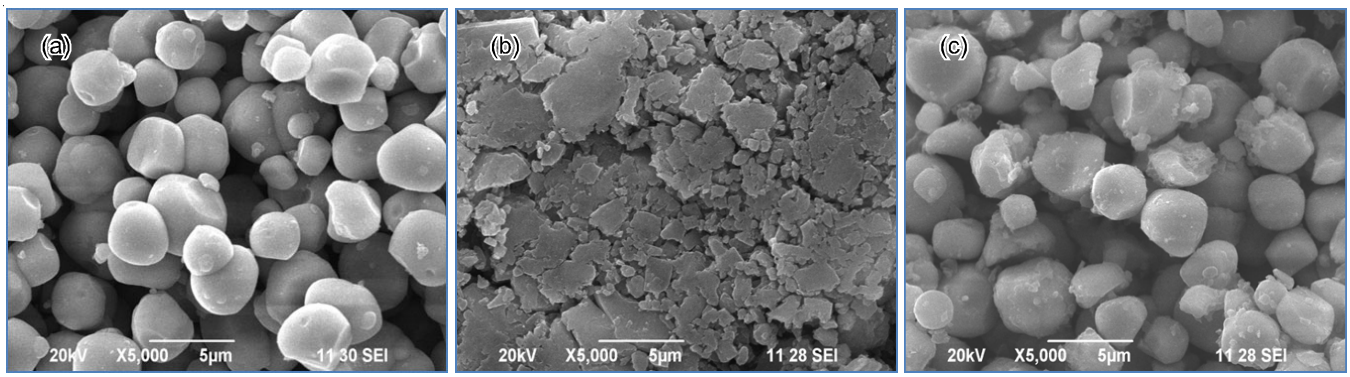

Fig. 7. SEM images of (a) HPA, (b) CDK and (c) [HPA(CDK)]

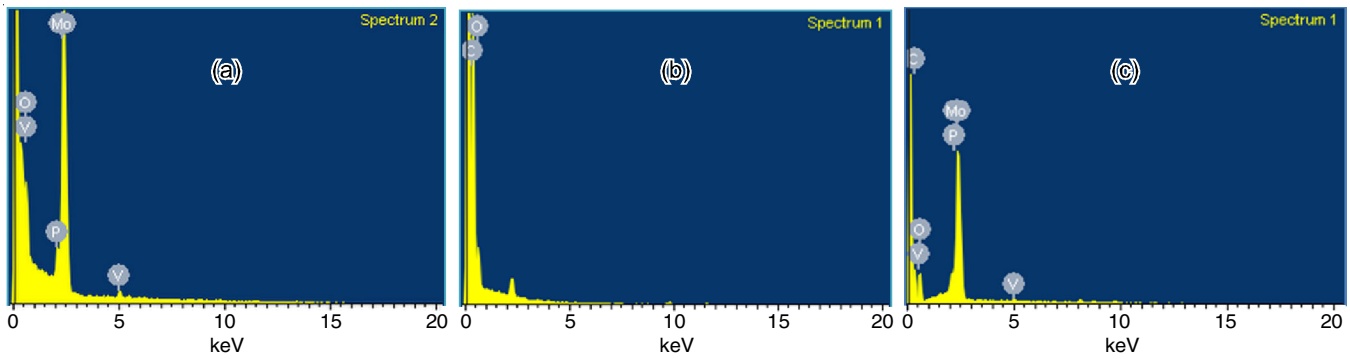

Fig. 8. EDS of (a) HPA, (b) CDK and (c) [HPA(CDK)]

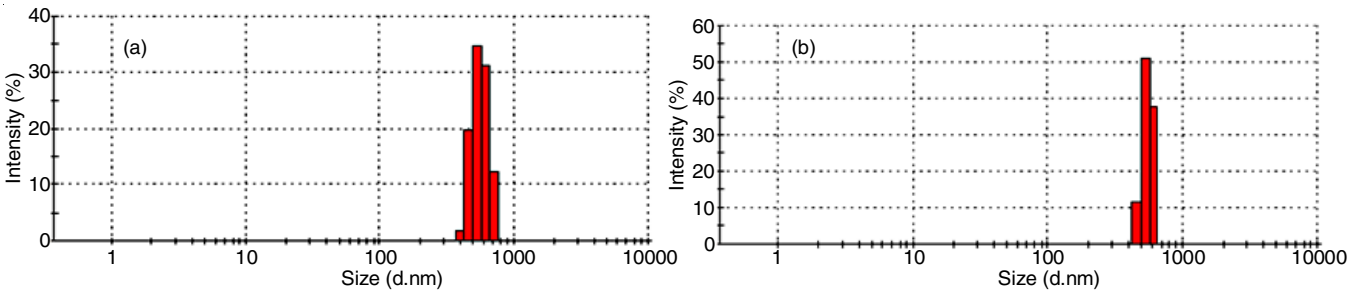

Fig. 9. DLS of (a) HPA and (b) [HPA(CDK)]

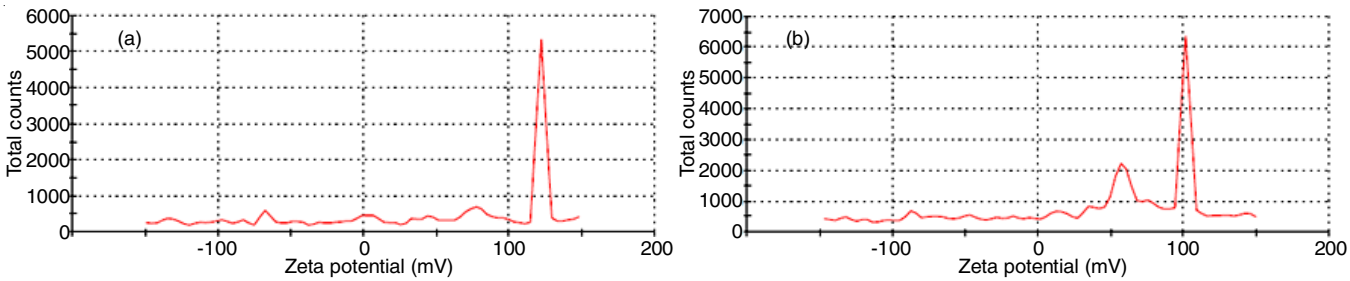

Fig. 10. Zeta potential of (a) HPA and (b) [HPA(CDK)]

Dynamic light scattering (DLS) and zeta potential: The DLS measurements of HPA and [HPA(CDK)] hybrid composite revealed a size of the organic-inorganic complex (Fig. 9). From Fig. 9a-b, the histogram shows the average size of the materials around 500-550 nm and broad size distributions. As shown in Fig. 10, both HPA and [HPA(CDK)] hybrid composite exhibited a positive charge of < 100-150 mV. The positive charge is due to the presence ion surfactant. Compared with HPA, results showed a slow increase in the zeta potential in negative charge of [HPA(CDK)]. The negative charge of hybrid material complex caused absorption of CDK on the HPA surface and conceal of negative charge in the surfactant. On the HPA surface with CDK shows a slight increase in zeta potential.

Thermal analysis: The DSC-TGA traces of HPA give the weight loss in the temperature range of 0-700 ºC (Fig. 11). The evaporation of residual water approximately (4.2%) between 10 and 200 ºC was assigned to the first and second weight loss [24,25]. The third and fourth weight loss (11.4%) associated in the temperature range of 220-553 ºC was might be due to the removal of oxides of vanadium, phosphorous and molybdenum oxides in the hybrid material.

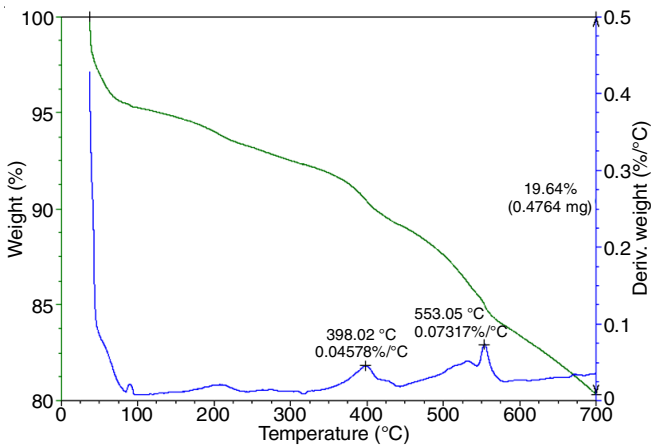

Fig. 11. DSC and TGA of HPA

The DSC-TGA traces of [HPA(CDK)] hybrid composite give the weight loss in the temperature range of 20-700 ºC (Fig. 12). The decomposition of imine groups in encapsulation and water molecules (7.8%) between 20 and 200 ºC correspond to first and second weight loss. The thermal stability has

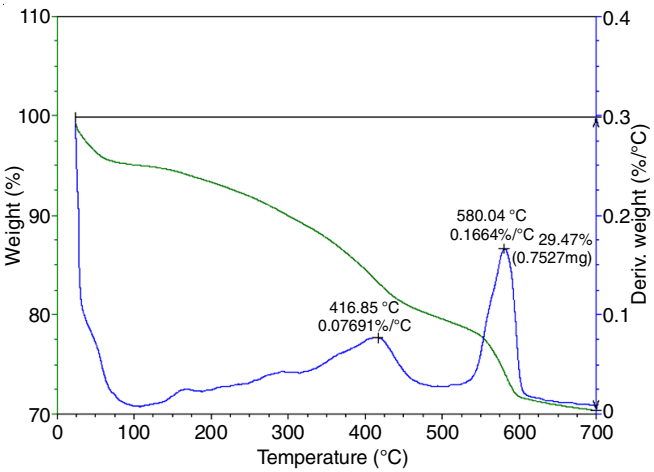

Fig. 12. DSC and TGA of [HPA(CDK)]

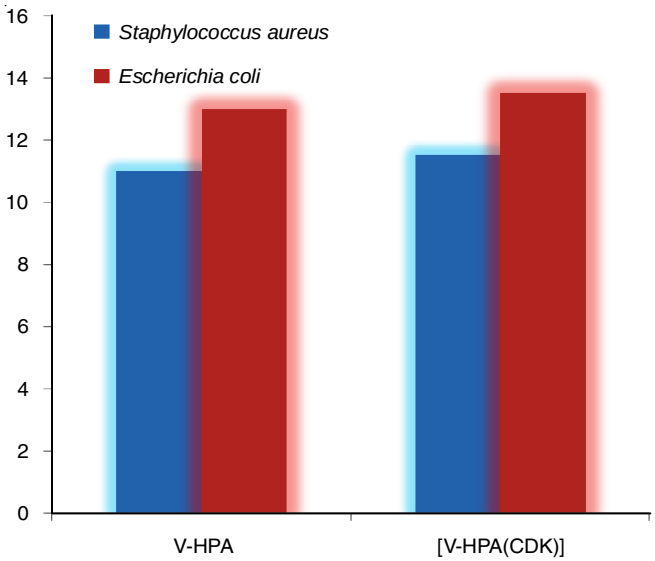

Fig. 13. Antimicrobial studies of (a) HPA and (b) [HPA(CDK)]

improved which attributes due to the presence of triazine ring in their structure. The third and fourth weight loss (20.4%) attributed in the temperature range of 210-580 ºC correspond to the multiple oxidative decomposition process [26].

Antimicrobial activity: The HPA and [HPA(CDK)] antimicrobial activity on *Staphylococcus aureus* and *Escherichia coli* is shown in Fig. 13. It is clear that the encapsulated organic-inorganic hybrid material [HPA(CDK)] shows better results than HPA. The [HPA(CDK)] responded much higher than HPA might be due to the bacterial properties of curcumin-benzoguanamine.

Anticancer activity: The [HPA(CDK)] cytotoxicity studies on MCF-7 cell lines showed a 85.5 % of cell death in the range

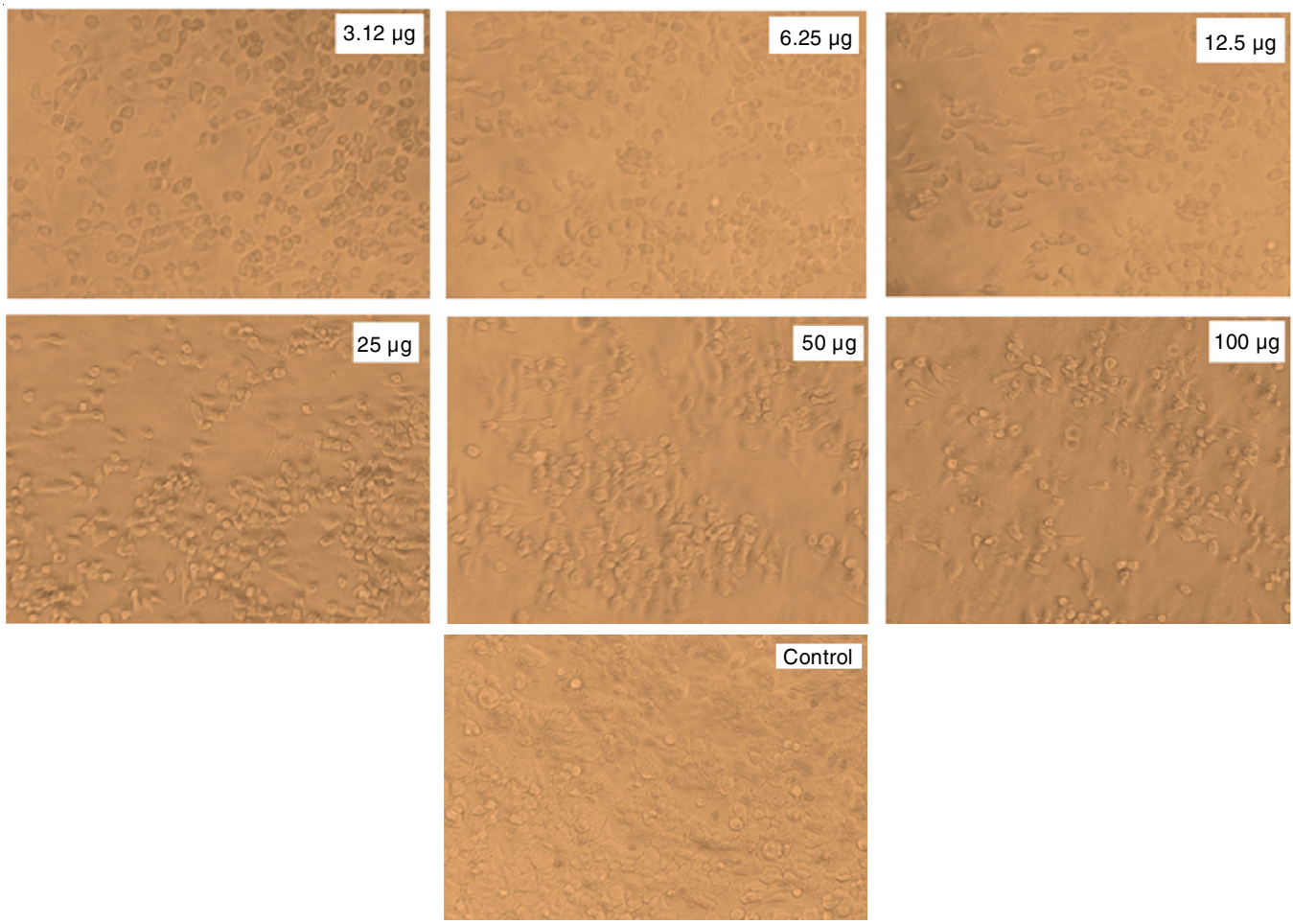

Fig. 14. Anticancer studies on MCF-7 cell lines of [HPA(CDK)]

of 3.12-100 µg/mL concentrations in 24 h at 37 ºC, 5% CO_2 incubator (Fig. 14). There is no sign of cell death in the untreated cell lines or blank. Table-5 shows the percentage of apoptosis at various concentrations. The anticancer activity of hybrid complex and microscopic images revealed the apoptosis of cancer cell. The anticancer studies for cisplatin were also compared to [HPA(CDK)] cytotoxicity studies on MCF-7 cell lines (Fig. 15). The curcumin-triazine matrix with active protons and reduction-oxidation reaction increase the oxidation states of the atom in HPA were responsible for higher cytotoxicity effect.

Conclusion

In summary, a novel composite of curcumin diketimine (CDK)-heteropolyacid (where HPA = vanadium doped Keggin anion and CDK = curcumin-benzoguanamine) was synthesized and characterized using spectral techniques *viz*. FTIR, ^{13}C NMR, SEM, EDS, XRD, thermal and ESR techniques. A SEM image represents a unique self-assembled round shape with size of a diameter around micro meter scale. The X-band EPR spectral data shows the 8 lines of hyperfine structure, which was due to the presence of V^{4+} ions in the HPA and [HPA(CDK)] composite. The *in vitro* anticancer studies showed that the promising viability (85.5 %) of [HPA(CDK)] against the cancer cell line of MCF-7 (breast cancer).

ACKNOWLEDGEMENTS

The financial support from the Don Bosco Research Grant, Sacred Heart College, Tirupattur, India is greatfully acknowledged.

CONFLICT OF INTEREST

The authors declare that there is no conflict of interests regarding the publication of this article.

TABLE-5
ANTI-CANCER ACTIVITY OF [HPA(CDK)]

Sample	Blank	MTT assay (MCF-7 cell line)						
		Concentration (µg)						
		Untreated	3.12	6.25	12.5	25	50	100
Reading 1	0.075	1.374	0.97	0.822	0.797	0.641	0.585	0.271
Reading 2	0.089	1.385	1.014	0.819	0.714	0.693	0.508	0.265
Reading 3	0.074	1.377	0.998	0.802	0.798	0.687	0.505	0.268
Mean	0.0793	1.378	0.994	0.8143	0.769	0.673	0.532	0.268
S.D		0.0056	0.0222	0.0107	0.0482	0.0284	0.0453	0.003
Viability %		100	70.359	56.567	53.129	45.741	34.889	14.520
							IC_{50} value = 13.28	

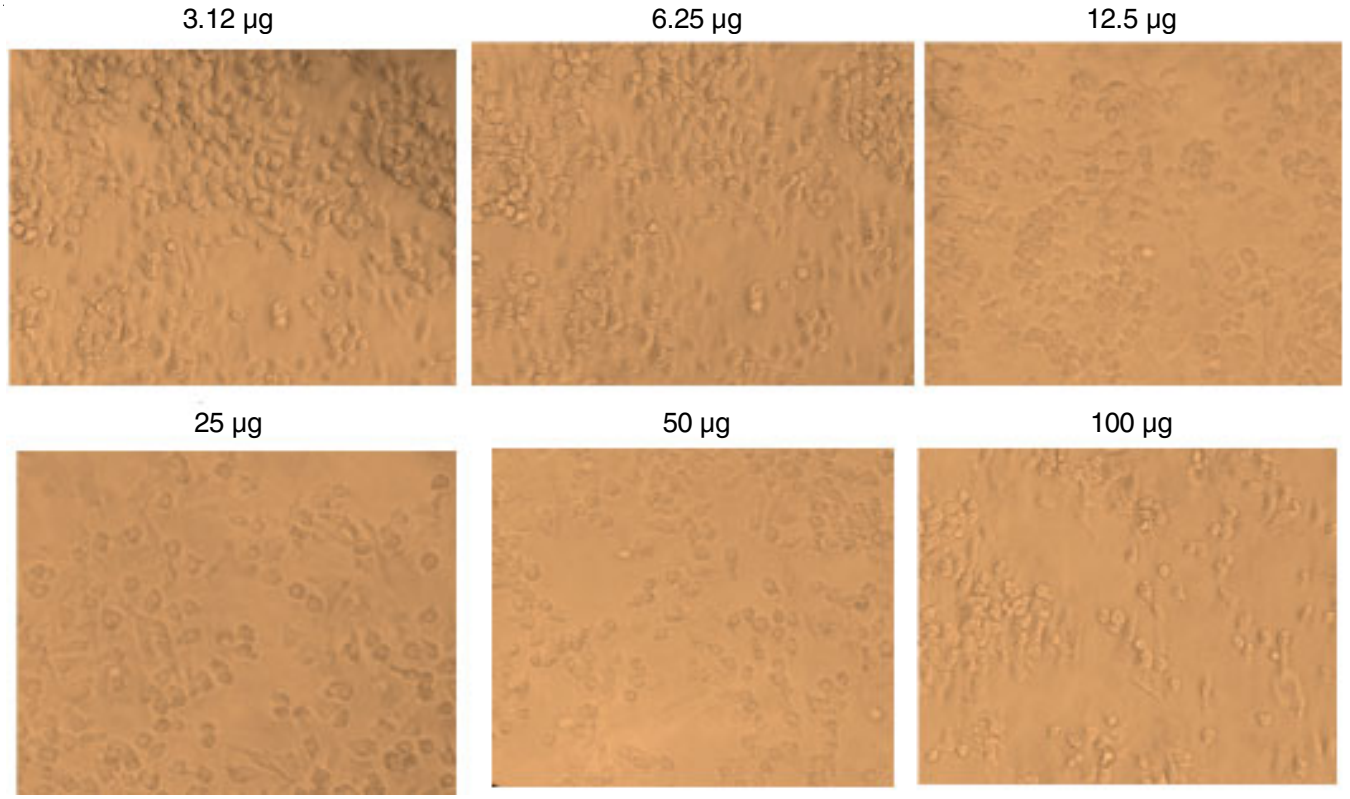

Fig. 15. Anticancer studies on MCF-7 cell lines of cisplatin

REFERENCES

1. N.S. Elbialy, *J. Adv. Phys.*, **16**, 185 (2019); https://doi.org/10.24297/jap.v16i1.8276
2. Azizullah, M. Al-Rashida, A. Haider, U. Kortz, S.A. Joshi and J. Iqbal, *ChemistrySelect*, **3**, 1472 (2018); https://doi.org/10.1002/slct.201702253
3. K. Girish, B. Channu and A.R. Baba, *Indian J. Pharm. Sci.*, **81**, 150 (2019); https://doi.org/10.4172/pharmaceutical-sciences.1000491
4. M. Jalali-Heravi, A.A. Khandar and I. Sheikshoaie, *Spectrochim. Acta A Mol. Biomol. Spectrosc.*, **55**, 2537 (1999); https://doi.org/10.1016/S1386-1425(99)00044-X
5. K. Rurack, J.L. Bricks, G. Reck, R. Radeglia and U. Resch-Genger, *J. Phys. Chem.*, **104**, 3087 (2000); https://doi.org/10.1021/jp994269k
6. Z. Xu, G. Bai and C. Dong, *Bioorg. Med. Chem.*, **13**, 5694 (2005); https://doi.org/10.1016/j.bmc.2005.06.023
7. S. Sumathi, P. Tharmaraj, C.D. Sheela and R. Ebenezer, *J. Coord. Chem.*, **65**, 506 (2012); https://doi.org/10.1080/00958972.2012.655727
8. M. Karimpour, M.A.H. Feizi, M. Mahdavi, B. Krammer, T. Verwanger, F. Najafi and E. Babaei, *Phytomedicine*, **57**, 183 (2019); https://doi.org/10.1016/j.phymed.2018.11.017
9. R. Duan, Z. Ou, W. Wang, S. Chen and X. Zhou, *Spectrochim. Acta A Mol. Biomol. Spectrosc.*, **151**, 64 (2015); https://doi.org/10.1016/j.saa.2015.05.063
10. F. Shen, Z.B. Ou, Y.J. Liu, W. Liu, B.-F. Wang, Z.-W. Mao and X.-Y. Le, *Inorg. Chim. Acta*, **465**, 1 (2017); https://doi.org/10.1016/j.ica.2017.05.030
11. M. Croce, S. Conti, C. Maake and G.R. Patzke, *Eur. J. Inorg. Chem.*, **2019**, 348 (2019); https://doi.org/10.1002/ejic.201800268
12. H. Cao, C. Li, W. Qi, X. Meng, R. Tian, Y. Qi, W. Yang and J. Li, *PLoS One*, **12**, e0181018 (2017); https://doi.org/10.1371/journal.pone.0181018
13. S. Wang and G.Y. Yang, *Chem. Rev.*, **115**, 4893 (2015); https://doi.org/10.1021/cr500390v
14. J. Kafawein, H.K. Juwhari and M.A. Al-Damen, *J. Cluster Sci.*, **26**, 1683 (2015); https://doi.org/10.1007/s10876-015-0867-9
15. S. Bharath, S. Jothi, P. Peter and T. Jeyabalan, *Int. J. Recent Scient. Res.*, **9**, 23480 (2018).
16. J. Arichi, M.M. Pereira, P.M. Esteves and B. Louis, *Solid State Sci.*, **12**, 1866 (2010); https://doi.org/10.1016/j.solidstatesciences.2010.01.022
17. K. Shakeela, G. Silpa, S.K. Rayala and G.R. Rao, *J. Chem. Sci.*, **130**, 107 (2018); https://doi.org/10.1007/s12039-018-1501-9
18. K. Sivakumar, G. Parinamachivayam, M.M. Krishnan, S. Chakravarty and A. Bharathi, *Spectrochim. Acta A Mol. Biomol. Spectrosc.*, **200**, 212 (2018); https://doi.org/10.1016/j.saa.2018.04.034
19. I. Kaminker, H. Goldberg, R. Neumann and D. Goldfarb, *Chem. Eur. J.*, **16**, 10014 (2010); https://doi.org/10.1002/chem.201000944
20. K. Geetha, A. Athira and N.J. Alummoottil, *Int. J. Pharm. Pharm. Sci.*, **6**, 171 (2014).
21. X. Liao, D. Wu, B. Geng, S. Lu and Y. Yao, *RSC Adv.*, **7**, 48454 (2017); https://doi.org/10.1039/C7RA08448J
22. W. Li, J. Xu, X. He, J. Zhang, E. Zong, X. Liu and S. Fu, *IOP Conf. Series Mater. Sci. Eng.*, **207**, 012015 (2017); https://doi.org/10.1088/1757-899X/207/1/012015
23. S.S. Hosseinyzade, F.M. Zonoz and B. Bahramian, *Catal. Lett.*, **148**, 1324 (2018); https://doi.org/10.1007/s10562-018-2354-z
24. R. Kitture, S. Ghosh, P.A. More, K. Date, S. Gaware, S. Datar, B.A. Chopade and S.N. Kale, *J. Nanosci. Nanotechnol.*, **15**, 4039 (2015); https://doi.org/10.1166/jnn.2015.10322
25. N. Kanagathara, N. Sivakumar, K. Gayathri, N.G. Renganathan, P. Krishnan, S. Gunasekaran and G. Anbalagan, *Proc. Indian Nat. Sci. Acad.*, **79**, 467 (2013).
26. A.P. Zambre, V.M. Kulkarni, S. Padhye, S.K. Sandur and B.B. Aggarwal, *Bioorg. Med. Chem.*, **14**, 7196 (2006); https://doi.org/10.1016/j.bmc.2006.06.056